P11R.5 QUANTITATIVE ANALYSIS OF WEATHER RADAR ATTENUATION CORRECTION ACCURACY

Alexis Berne* and Remko Uijlenhoet
Environmental Sciences, Wageningen University, The Netherlands

1 INTRODUCTION

At short wavelengths (e.g. C- and X-band), the attenuation of the radar signal by the precipitation along its path is a critical issue for quantitative radar rain estimates that has been recognized for a long time (e.g. Hitschfeld and Bordan, 1954). A recently developed stochastic simulator of range profiles of raindrop size distributions (DSD) provides a controlled experiment framework to investigate the accuracy and robustness of attenuation correction algorithms (Berne and Uijlenhoet, 2005).
This paper focuses on the quantification of the influence of uncertainties concerning the radar calibration, the parameterization of a power-law relation between the radar reflectivity Z and the specific attenuation k, and total path integrated attenuation (PIA) estimations. The analysis concerns single frequency, incoherent and non-polarimetric radar systems. Two attenuation correction algorithms are studied: a forward algorithm based on the analytical solution proposed by Hitschfeld and Bordan (1954) and a backward algorithm based on the solution proposed by Marzoug and Amayenc (1994). From DSD range profiles, the corresponding profiles of bulk rain variables are derived. Using a Monte Carlo approach, the accuracy of the two algorithms is quantified for the different sources of error previously mentioned.

2 DSD SIMULATOR

The DSD simulator used in the following has been proposed by Berne and Uijlenhoet (2005). It enables to generate realistic DSD range profiles. It is based on the exponential DSD, which two parameters N_t and λ are considered to be random variables

$$N(D|N_t, \lambda) = N_t \, \lambda \, e^{-\lambda D} \, , \tag{1}$$

where $N(D|N_t, \lambda)dD$ denotes the drop concentration in the diameter interval $[D, D + dD]$ given N_t and λ. The latter are assumed to be jointly lognormally distributed and their logarithms are assumed to follow a bivariate first order vector auto-regressive process. Assuming Taylor's hypothesis with a constant velocity of 12.5 m s^{-1} (see Berne and Uijlenhoet, 2005), the parameters have been derived from DSD measurements for an intense rain period of 45 minutes, collected during the HIRE'98 experiment in Marseille, France (see Table 1).

Table 1: Mean, standard deviation and characteristic time of $N' = \ln N_t$ and $\lambda' = \ln \lambda$ deduced from HIRE'98 data at a 60 s time step.

	Mean	Std	θ (s)
N'	7.49	0.44	430
λ'	0.88	0.32	430

The generated DSD profiles have a total length of 30 km, with a spatial resolution of 25 m. From these DSD profiles, the corresponding profiles of bulk rain variables (e.g. R, Z and k) are easily derived. This controlled experiment framework allows to apply a Monte Carlo technique to quantify the respective influence of the different sources of uncertainty in attenuation correction.

3 ATTENUATION CORRECTION ALGORITHMS

As mentioned in the introduction, we consider incoherent, single frequency and non-polarimetric radar systems. Two different types of algorithms will be studied in the following. The measured attenuated reflectivity Z_a reads

$$Z_a(r) = \delta_c A(r) Z(r) \, , \tag{2}$$

where δ_c is the calibration error factor and $A(r)$ is the two-way attenuation factor at the range r ($0 \leq A \leq 1$). Assuming the Z-k relation reads

$$Z = \delta_\alpha \alpha \, k^{\delta_\beta \beta} \, , \tag{3}$$

where δ_α (δ_β respectively) is the error factor in α (β). Therefore, A can be written as

$$A(r) = \exp\left[-0.2\ln(10)\int_0^r \left(\frac{Z(s)}{\delta_\alpha \alpha}\right)^{1/(\delta_\beta \beta)} ds\right] . \tag{4}$$

* *Corresponding author address:* Alexis Berne, Environmental Sciences, Nieuwe Kanaal 11, 6709 PA Wageningen, The Netherlands; e-mail: Alexis.Berne@wur.nl

Hitschfeld and Bordan (1954) (HB hereafter) proposed an analytical solution to express Z as a function of Z_a:

$$Z(r) = Z_a(r) / \left[\delta_c^{1/(\delta_\beta \beta)} - \frac{0.2 \ln(10)}{\delta_\beta \beta} \int_0^r \left(Z_a(s)/\delta_\alpha \alpha\right)^{1/(\delta_\beta \beta)} \, ds \right]^{\delta_\beta \beta} . \quad (5)$$

The HB algorithm is a forward algorithm because the integral is between 0 and r. However, the difference in its denominator can be close to 0 and this makes the algorithm highly unstable.

To avoid instability problems, another family of attenuation correction algorithms has been developed. It is based on the knowledge of an estimate A_0 of the PIA at a given range r_0. The estimate A_0 can be uncertain, that is

$$A(r_0) = \delta_A A_0 , \quad (6)$$

where δ_A is the error factor in A_0. The reformulation of Eq.(5) starting from r_0 and going backward to the radar guarantees the stability of the algorithms. As an example, we use the solution proposed by Marzoug and Amayenc (1994) (MA hereafter):

$$Z(r) = Z_a(r) / \left[(\delta_c \delta_A A_0)^{1/(\delta_\beta \beta)} + \frac{0.2 \ln(10)}{\delta_\beta \beta} \int_r^{r_0} \left(Z_a(s)/\delta_\alpha \alpha\right)^{1/(\delta_\beta \beta)} \, ds \right]^{\delta_\beta \beta} . \quad (7)$$

The main drawback of such a backward algorithm is that it requires a reliable estimation of the PIA at a given range.

To study the accuracy of the algorithms, we use a Monte Carlo technique. The analysis focuses on attenuation correction using Eqs. (5) and (7). One thousand profiles of N_t and λ (hence of Z, k and Z_a) are generated. To be consistent with operational radar sampling resolutions, the high spatial resolution (25 m) profiles are averaged at a lower spatial resolution of 250 m. On each profile a Z-k power-law relation is fitted by means of a non-linear regression technique. It must be noted that they constitute the best possible power-law relations. The exact PIA value is calculated as the difference between the non-attenuated and the attenuated Z profiles. Then the two algorithms are applied using the fitted relations on the 1000 profiles.

Figure 1 shows the median, as well as the 10% and 90% quantiles, of the distribution of the root mean square error (RMSE) calculated between the exact Z profiles and the Z_c profiles obtained by applying the two attenuation correction algorithms without any uncertainty (i.e. $\delta_c = \delta_\alpha = \delta_\beta = \delta_A = 1$). The

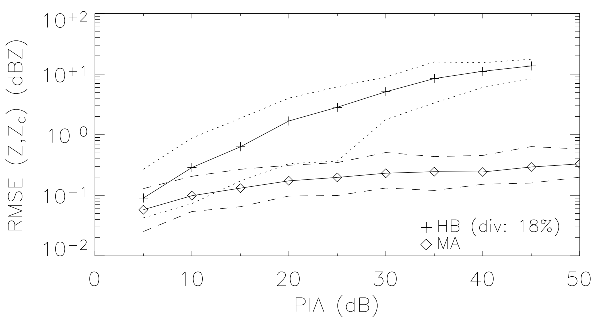

Figure 1: Median (solid line) of the distribution of the RMSE calculated between the exact Z profiles and the Z_c profiles obtained by applying the two attenuation correction algorithms, for 1000 profiles at a 250 m resolution. The dotted (dashed) lines represent the 10% and 90% quantiles for the HB (MA) algorithm. 'div' indicates the percentage of diverging HB corrections. The convention is the same for the subsequent figures.

significant dispersion of the distribution (Fig. 1 is in log scale) is explained by the fact that the use of a deterministic power law between Z and k is not fully consistent with the stochastic nature of these variables.

Obviously, the MA algorithm ($0.05 <$ median $<$ 0.3 dBZ) is more stable and accurate than the HB algorithm ($0.05 <$ median < 10 dBZ), which diverges in about 1 in 5 cases. These RMSE values will constitute the reference values for the quantification of the influence of the different sources of uncertainty, as detailed in the following sections.

4 INFLUENCE OF THE UNCERTAINTY IN CALIBRATION

Radar systems can be affected by calibration errors. In this section, the influence of the uncertainty in calibration on the accuracy of the attenuation correction algorithms is quantified. For better visual inspection, the calibration error is expressed in dBZ as $\epsilon_c = 10 \log(\delta_c)$ and varies in the interval [-5,+5]. The additional error due to uncertain calibration is calculated as the ratio between the RMSE values for a given calibration error and the reference RMSE values. Figure 2 presents the median, as well as the 10% and 90% quantiles, of the distribution of RMSE ratio as a function of the calibration error.

The other error factors (δ_α, δ_β and δ_A) are fixed to 1. When $\epsilon_c > 0$, the median values are similar for

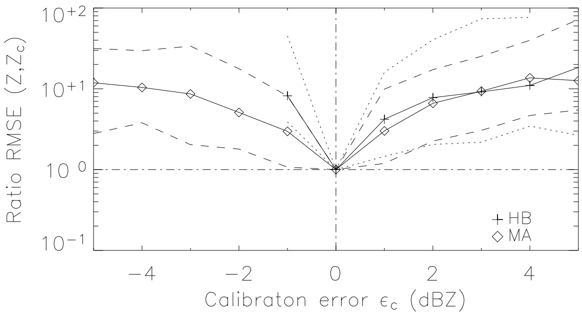

Figure 2: Median, 10% and 90% quantiles of the distribution of the RMSE ratio as a function of the calibration error ϵ_c expressed in dBZ, for the two attenuation correction algorithms.

the two algorithms but the dispersion is larger for the HB algorithm. When $\epsilon_c > 0$, the distribution remains similar for the MA algorithm. For the HB algorithm, Eq. 5 shows that $\delta_c < 1$ (or $\epsilon_c < 0$) results in more diverging profiles because the denominator can be close to zero for smaller Z_a values, as illustrated in Fig. 2 by the sharp increase of the median when $-1 < \epsilon_c < 0$ and the divergence of the algorithm when $\epsilon_c < -1$ (absence of points).
As expected, the RMSE ratio rapidly increases when $\epsilon_c \neq 0$, that is the calibration error decreases significantly the accuracy of the two algorithms. For instance, the median RMSE ratio value is about 3 when $\epsilon_c = \pm 1$ for the MA algorithm. It is about 4 (8 respectively) when $\epsilon_c = +1$ (-1).

5 INFLUENCE OF THE UNCERTAINTY IN THE PARAMETERIZATION OF THE Z-K RELATION

The two studied algorithms are based on the assumption of a power-law relation between Z and k. To analyze the influence of the uncertainty in the parameters of the Z-k power law on the accuracy of the two attenuation correction algorithms, an error factor between 0.7 and 1.3 is applied to the prefactor (the exponent respectively). The additional error due to uncertain parameterization of the Z-k relation is calculated as the ratio between the RMSE values for a given prefactor (exponent) error and the reference RMSE values. Figure 3 presents the median, as well as the 10% and 90% quantiles, of the distribution of the RMSE ratio as a function of the relative deviation of the prefactor and exponent, with respect to the reference Z-k relation. The other error factors (δ_c and δ_A) are fixed to 1. For the pref-

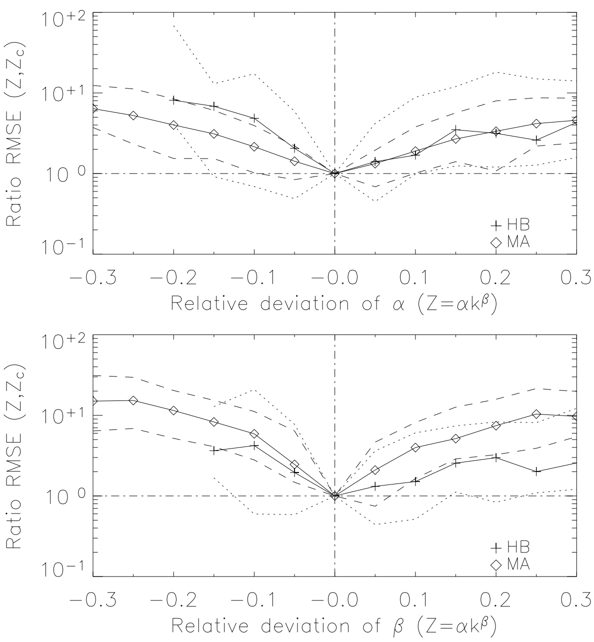

Figure 3: Median, 10% and 90% quantiles of the distribution of the RMSE ratio as a function of the relative deviation of the prefactor (top panel) and exponent (bottom panel) of the Z-k power law, for the two attenuation correction algorithms.

actor (top panel of Fig. 3), the distribution of the RMSE ratio is very similar for the two algorithms when $\delta_\alpha > 1$. However, the HB algorithm is more sensitive to the error in α when $\delta_\alpha < 1$, which is consistent with Eq. (5). For instance, the median RMSE ratio is about 3 when the error is about $\pm 20\%$ in the prefactor for the MA algorithm. It is about 3 (7 respectively) when the error is about 20% (-20%) for the HB algorithm.
The influence of the exponent is stronger for both algorithms, as indicated by the higher values of the RMSE ratio. It must be noted that the MA algorithm is more sensitive to the error in β. For instance, the median RMSE ratio is about 9 when the error in the exponent is about 20% for the MA algorithm. It is about 3 when the error is about 20% for the HB algorithm.

6 INFLUENCE OF THE UNCERTAINTY IN THE PIA ESTIMATE

The MA algortihm is more accurate and more robust than the HB algorithm, but it requires an additional parameter which is the estimate of the PIA at a given range. This section is devoted to the quantification of the influence of the uncertainty in this PIA estimate on the accuracy of the MA algorithm.

Similarly to ϵ_c, we define $\epsilon_A = 10\ \log(\delta_A)$. The error in the PIA estimate ϵ_A is generated as a Gaussian white noise with a standard deviation of 2.5 dB (Delrieu et al., 1999). The additional error due to uncertain PIA estimate ϵ_A is calculated as the ratio between the RMSE values for the uncertain PIA estimate and the reference RMSE values. Figure 4 presents the median, as well as the 10% and 90% quantiles, of the distribution of the RSME ratio as a function of ϵ_A for the MA algorithm. The other error factors (δ_c, δ_α and δ_β) are fixed to 1. According

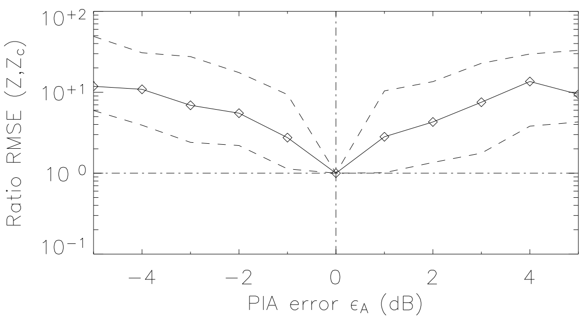

Figure 4: Median, 10% and 90% quantiles of the distribution of the RMSE ratio as a function of the PIA error ϵ_A expressed in dB for the MA algorithm.

to Eq. (7), Fig. 4 and Fig. 2 should be identical because δ_A and δ_c can be interchanged. In fact, for a given reference Z_a profile, the error in the calibration and in the PIA estimate are generally different and therefore the deduced distribution of the RMSE ratio is slightly different. Nevertheless, the influence of δ_A is the same as δ_c.

7 CONCLUSIONS

Attenuation correction is an important step for quantitative rain estimation using C- or X-band weather radar. In this paper, we focus on X-band incoherent, single frequency and non-polarimetric radar systems. We investigate the influence of uncertainties in the radar calibration, in the parameterization of a power-law relation between the radar reflectivity Z and the specific attenuation k, and in the total path integrated attenuation (PIA) estimates on the accuracy of two attenuation correction algorithms. The first (HB algorithm) is based on a forward implementation and is known for its instability. The second (MA algorithm) is based on a backward implementation and is stable, but requires an additional piece of information which is the PIA at a given range from the radar. A stochastic model of DSD range profiles provides a controlled experiment framework, with fully consistent Z and k profiles, to quantify the influence of the different sources of uncertainty. An uncertainty of 1 dBZ in the measured Z (or of 1 dB in the PIA estimate) leads to a multiplication of the RMSE by at least a factor 3. An uncertainty of about 20% in the prefactor (exponent respectively) leads to a multiplication of the RMSE by at least a factor 5 (2). The influence of the use of alternative DSD models (e.g. gamma, lognormal) is the subject of ongoing research.

Acknowledgments. This research is supported by the EU projects FLOODSITE and VOLTAIRE. The second author is also supported by the Netherlands Organization for Scientific Research (NWO).

REFERENCES

Berne, A. and R. Uijlenhoet, 2005: A stochastic model of range profiles of raindrop size distributions: application to radar attenuation correction. *Geophys. Res. Lett.*, **32**, doi:10.1029/2004GL021899.

Delrieu, G., S. Serrar, E. Guardo, and J.-D. Creutin, 1999: Rain measurement in hilly terrain with X-band weather radar systems: accuracy of path-integrated attenuation estimates derived from mountain returns. *J. Atmos. Oceanic Technol.*, **16**, 405–415.

Hitschfeld, W. and J. Bordan, 1954: Errors inherent in the radar measurement of rainfall at attenuating wavelengths. *J. Meteor.*, **11**, 58–67.

Marzoug, M. and P. Amayenc, 1994: A class of single- and dual- frequency algorithms for rain-rate profiling from a spaceborne radar. Part I: principle and tests from numerical simulations. *J. Atmos. Oceanic Technol.*, **11**, 1480–1506.